Eur. Phys. J. D **2**, 33–39 (1998)

THE EUROPEAN PHYSICAL JOURNAL D

Isotope shifts and hyperfine structure in the 3d $^2D_J \rightarrow$ 4p ^2P_J transitions in calcium II

W. Nörtershäuser[a], K. Blaum, K. Icker, P. Müller, A. Schmitt, K. Wendt, and B. Wiche

Institut für Physik, Johannes Gutenberg-Universität Mainz, 55099 Mainz, Germany

Received: 19 September 1997 / Revised: 5 December 1997 / Accepted: 27 January 1998

Abstract. The isotope shift and hyperfine structure in the three 3d $^2D_{3/2,5/2} \rightarrow$ 4p $^2P_{1/2,3/2}$ - transitions in Ca II have been studied by fast ion beam collinear laser spectroscopy for all stable Ca isotopes. The metastable 3d states were populated within the surface ionization source of a mass separator with a probability of about 0.1%. After resonant excitation to the 4p levels with diode laser light around 850 nm the uv photons from the 4p $\rightarrow$ 4s transitions to the ground state were used for detection. Hyperfine structure parameters A and B for the odd isotope ^{43}Ca, as evaluated from the splittings observed, agree well with theoretical predictions from relativistic many-body perturbation theory. Field shift constants K^{FS} and specific mass shift constants K^{SMS} were extracted from the measured isotope shifts and are discussed in comparison with expectation values from theory.

PACS. 32.10.Fn Fine and hyperfine structure

1 Introduction

As a member of the alkaline earth elements, calcium has been the subject of various spectroscopic studies during the last decades including precise hyperfine structure and isotope shift investigations in a number of optical transitions in both the atomic and ionic spectrum [1–4]. There are different reasons for this interest in the atomic structure of calcium in addition to revealing insight into the nuclear structure of this element. Singly positive charged ions of the alkaline-earth elements have a simple alkali-metal like electronic structure, consisting of an inert-gas-like electron core and a single valence electron. Hence, calculations on the atomic structure can be carried out using a number of different theoretical methods including ab-initio calculations and semi-empirical approaches, which give more or less precise predictions for the parameters involved in the experimental spectra like term energies, isotope shift and hyperfine structure constants. The hyperfine structure of the low-lying atomic states, particularly the 4s, 4p and 3d levels has been accurately predicted by refined many-body perturbation theory (MBPT) including core polarization and correlation effects [5]. In the case of the 4s and 4p levels these values have recently been confirmed by different experimental measurements [2,3].

As discussed by Mårtensson-Pendrill [3], particularly the 3d states are of special importance for a test of the validity of these refined MBPT evaluations because core polarization and correlation effects have a rather strong impact on these levels as compared to the 4s and 4p states. In addition to these effects, the 3d electron is expected to exhibit a pronounced influence on correlations within the core due to its relatively high charge density inside the core. So far only a single measurement of one of the magnetic dipole hyperfine structure constants has been reported with a value of $A(3d\ ^2D_{3/2}) = -48.3(1.6)$ MHz [4], which is in reasonable agreement with the theoretical predictions. To our knowledge precise results for the $A(3d\ ^2D_{5/2})$ and both $B(3d)$ factors have not been published, while experimental values for the 4p-states reported in the literature are contradictionary [2,6]. The relevant part of the Ca II level scheme is sketched in Figure 1, including all allowed electric dipole transitions between the levels concerned.

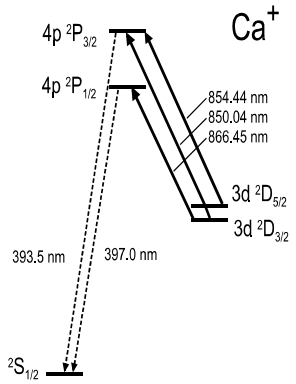

Fig. 1. Partial level scheme of Ca II.

[a] e-mail:
W.Noertershaeuser@larissa.physik.uni-mainz.de

One motivation for isotope shift studies in the 3d → 4p transitions in Ca II is the completion of the high-resolution measurements on isotope shifts in the different transitions connecting the 4s, 4p and 3d states. Here, a complete set of precise experimental results for the field shift and the specific mass shift factors are demanded *e.g.* in [3] for comparison to the theoretical description by MBPT. Experimental results for the 4s → 4p singlet transitions again are in good agreement. The predicted field shift factor $K_{3d}^{FS} = +110(1)$ MHz/fm^2 has already been used in [4] to separate the specific mass shift contribution from the isotope shift, but its value has not yet been confirmed by measurements.

Apart from these atomic physics studies, high resolution laser spectroscopy in the Λ-type system between the low-lying levels in Ca II has important applications for metrological investigations. In particular, the forbidden 4s $^2S_{1/2} \rightarrow$ 3d $^2D_{3/2,5/2}$ electric quadrupole transitions at 729 nm and 732 nm, respectively, and the 3d $^2D_{3/2} \rightarrow$ 3d $^2D_{5/2}$ M1-transition at 1.8 GHz are promising candidates for the development of an ultraprecise frequency standard. All transitions in the Λ-type excitation scheme of Ca II have the unique advantage that the required wavelengths for state preparation and optical cooling can be generated easily by solid-state diode lasers and furthermore have very narrow natural linewidths [7]. For these applications the precise knowledge of the isotope shifts and especially the hyperfine structure splittings of the only stable odd-mass isotope ^{43}Ca in all levels involved is desirable for precise laser tuning.

In this paper we report the study of the isotope shifts in the three allowed 3d $^2D_{3/2,5/2} \rightarrow$ 4p $^2P_{1/2,3/2}$ transitions for all stable isotopes of calcium and of the hyperfine structure of ^{43}Ca (I=7/2). The measurements have been carried out using fast ion beam collinear laser spectroscopy. Direct population of the 3d states in a surface ionization source has been utilized, avoiding the use of a second laser for state preparation by optical pumping. Field shift constants, specific mass shift constants and all hyperfine constants A and B of the levels involved are derived and compared to the theoretical predictions.

2 Experimental procedure

Collinear laser spectroscopy on fast beams of ions or atoms has become a standard experimental procedure for the investigation of isotope shifts and hyperfine structures. Up to now it has been applied to a large number of stable and radioactive isotopes from all over the nuclid chart [8]. The method combines a number of striking advantages, which are only partly accessible by other experimental techniques: The direct investigation of an ion beam from a mass separator avoids sample preparation and handling, and implies long interaction time as well as high excitation efficiency. The Doppler width of the optical transition is strongly reduced during the acceleration of the ions, allowing for high-resolution studies near to the natural linewidth limit. In addition to this, high sensitivity is achieved by involving all ions or atoms in the optical excitation, thus enabling the analysis of low abundance trace isotopes or artificially produced short-lived radioisotopes. Doppler tuning of the frequency can easily be performed by changing the acceleration potential without the necessity of precise laser frequency tuning. Most important for our work is the direct access to metastable states, which can be populated either during a charge exchange process or directly in the mass separator ion source. In the spectrum of Ca II the method has previously been used for high-resolution studies in the 4s $^2S_{1/2} \rightarrow$ 4p $^2P_{1/2,3/2}$ transitions [3]. In the spectrum of Ca I a variety of precision measurements has also been performed using other methods either in the strong 4s^2 $^1S_0 \rightarrow$ 4s4p $^1P_1$ transition ([9] and references therein) or in the 4s^2 $^1S_0 \rightarrow$ 4s4p $^3P_1$ intercombination line ([10–12] and references therein). Also these measurements cover long sequences of stable and radioactive isotopes and give precise $\delta\langle r^2\rangle$ values and nuclear moments. Furthermore the development of isotope shifts in the 4s nd series has been studied [13].

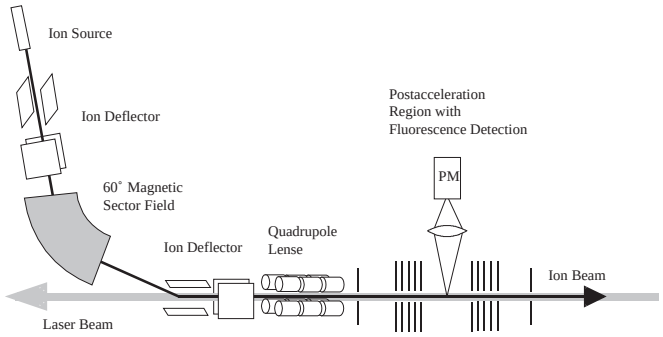

Fig. 2. Experimental setup for fast ion beam collinear laser spectroscopy.

A schematic diagram of our experimental setup is shown in Figure 2.

It is divided into four major parts: the ion source, the mass separator, the apparatus for collinear laser spectroscopy with the fluorescence detection region, and the laser setup. The Ca^+ ions are efficiently produced from $Ca(NO_3)_2$ in a surface ionization source of the Dubna type [14]. After reduction and atomization in a tantalum oven, the calcium atoms are ionized in a 2500 °C tungsten tube and extracted into the mass separator by a 35 kV potential. Typical Ca^+ beam currents are 500 nA. The high temperature in the ion source leads to a thermal population of the metastable 3d states of about 0.1%. Mass separation is accomplished in a 60° sector magnet. A 10° electrostatic deflector is used to superimpose the ion beam onto the laser beam in strict antiparallel geometry. To avoid depopulation of the 3d state by laser excitation before reaching the detection region, the laser frequency is tuned several GHz below the resonance frequency. A postacceleration potential of up to ±10 kV within the detection chamber allows for precise Doppler tuning into resonance. Fluorescence detection is performed by single-photon counting on a 4 cm long part of the beam with an

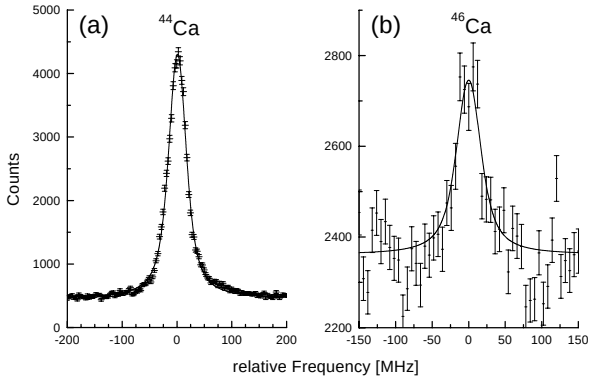

Fig. 3. Experimental data points with statistical error bars and Voigt-profile fit for ^{44}Ca (a) and ^{46}Ca (b) in the transition 3d $^2D_{5/2} \rightarrow$ 4p $^2P_{3/2}$.

estimated detection efficiency of approximately 3×10^{-3}. The use of a photomultiplier, which is sensitive only in the blue spectral region with very low efficiency for infrared photons eliminates background from laser stray light. The laser system consists of a diode laser in an external Littrow geometry resonator which is actively stabilized to a commercial stabilized Helium-Neon-laser by a 300 MHz reference etalon and comparison of the fringing pattern by a computer. The laser is operated at an output power of 5 mW and has a linewidth of 3 MHz, limited by acousto-mechanical noise. Using the external resonator together with precise current and temperature control, the diode laser can be tuned and stabilized at the wavelengths of all three 3d $\rightarrow$ 4p transitions around 850 nm, 854 nm, and 867 nm, respectively. Single-photon counts are recorded as a function of the postacceleration voltage with stabilized laser frequency. Alternatively laser scans were applied to test the precision of the acceleration voltage. Measurements of all stable isotopes in all three 3d $\rightarrow$ 4p transitions were performed with respect to the most abundant isotope ^{40}Ca to minimize the influence of voltage or frequency drifts. A signal for the rare isotope ^{46}Ca (natural abundance 3×10^{-5}) was observed only in the strongest 3d $^2D_{5/2} \rightarrow$ 4p $^2P_{3/2}$ transition.

3 Experimental results and discussion

3.1 Resonance peak positions and shapes

We determined the peak positions of the even isotopes from the experimental data by fitting a Voigt profile to the experimental observed resonance curve, which contains natural lifetime (lorentzian) and residual Doppler (gaussian) components. A typical example is shown in Figure 3a for the isotope ^{44}Ca.

The obtained Voigt linewidths (FWHM) of the resonances are 40(2) MHz for the less abundant isotopes of calcium and 54(2) MHz for the dominant isotope ^{40}Ca. In both cases the lorentzian contributions to the total widths are similar at 30(3) MHz, which compares well to the natural linewidth of 23 MHz and an additional 5 MHz of transit time broadening. The gaussian contribution varies from 22(3) MHz to 34(3) MHz, respectively. The reason for this discrepancy is partly ascribed to space charge effects in the intense ^{40}Ca beam, and saturation effects in the photomultiplier and the subsequent counting electronics, as no dead-time correction has been applied. Nevertheless, the uncertainty in the peak positions resulting from the fitting procedure is smaller than 1 MHz in both cases. This precision is verified by comparison of the center frequency for the isotopes performed over a period of two hours. Under all experimental conditions the long term variation was less than 2.5 MHz, reflecting the good frequency stability of the stabilized diode laser. Because of the low signal-to-noise-ratio for the least abundant isotope ^{46}Ca, all recorded scans of this isotope were added and a Voigt profile was fitted to the sum with gaussian and lorentzian linewidths fixed to the values determined for the other minor isotopes. The result is shown in Figure 3b. The uncertainty of the line center for this spectrum was pessimistically estimated to amount to 5 MHz.

3.2 Hyperfine structure of the odd isotope ^{43}Ca

^{43}Ca is the only stable odd isotope of calcium with a non vanishing nuclear spin (I=7/2). Magnetic dipole and electric quadrupole interactions between the core and the nucleus leads to a hyperfine splitting of all atomic states with non-vanishing angular momentum J. The size of the energy shift for the different hyperfine structure components relative to the center of gravity is given by the well-known formula [15]

$$\Delta E = \frac{A}{2}C + B\frac{\frac{3}{4}C(C+1) - I(I+1)J(J+1)}{2(2I-1)(2J-1)IJ} \qquad (1)$$

where $C = F(F+1) - I(I+1) - J(J+1)$ is the Casimir factor, $A = \dfrac{\mu_I H_e(0)}{IJ}$ the magnetic dipole coupling constant and $B = eQ_s\phi_{ij}(0)$ the electric quadrupole coupling constant. $H_e(0)$ and $\phi_{ij}(0)$ are the magnetic field and the electric-field gradient produced by the electrons at the nucleus. Different scans over the ^{43}Ca hyperfine structure have been added to form an experimental hyperfine spectrum as shown in Figure 4.

Included in the figure are the positions and intensities of the individual hyperfine components as derived from a fitting routine given below. The hyperfine structure of the 3d state is not fully resolved in all cases. This problem is most pronounced for the 3d $^2D_{5/2} \rightarrow$ 4p $^2P_{3/2}$ transition. Hence a sophisticated fitting routine was needed to deliver reasonable experimental A and B factors from the observed hyperfine structure patterns. Voigt profiles with identical gaussian as well as lorentzian linewidths for all components were interconnected by the hyperfine structure formula assuming theoretical intensity ratios. Any change of intensity ratios by hyperfine pumping is negligible because less then 10% of the excited atoms in the 4p state decay back to a 3d state. With this function a χ^2 minimization was performed comparing the calculated

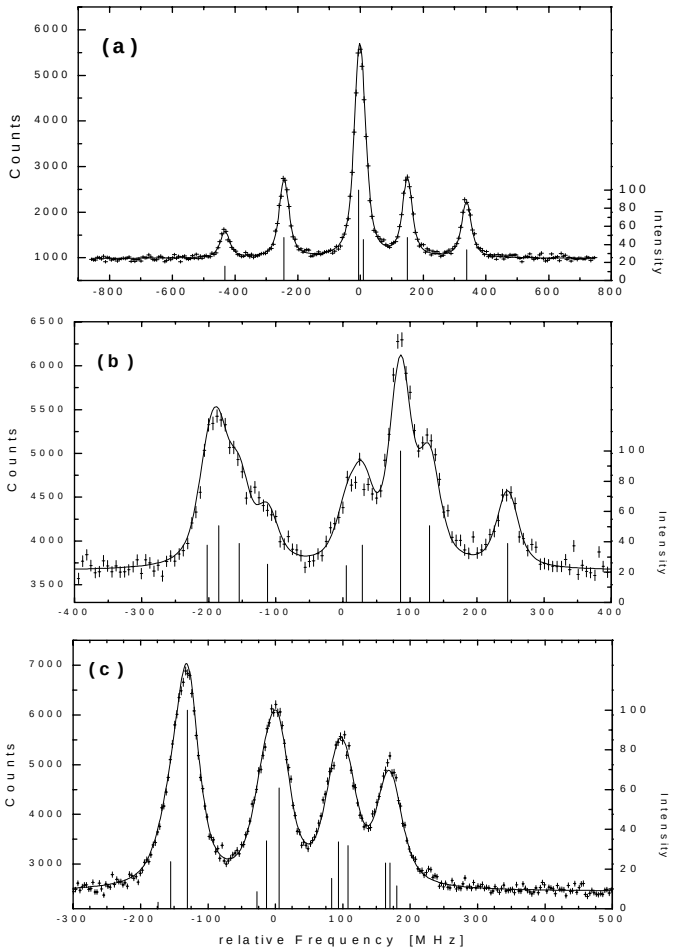

Fig. 4. Experimental hyperfine structure data with statistical error bars, fit curve, hyperfine transition positions, and intensities. (a) 3d $^2D_{3/2} \rightarrow$ 4p $^2P_{1/2}$, (b) 3d $^2D_{3/2} \rightarrow$ 4p $^2P_{3/2}$, (c) 3d $^2D_{5/2} \rightarrow$ 4p $^2P_{3/2}$.

pattern with the experimental data. Variable parameters in the fitting procedure were: the A and B factors of the states involved, gaussian and lorentzian linewidths, overall intensity, isotope shift of the center of gravity and a baseline offset (noise). The error of each data point was assumed to be purely statistical. With the theoretical hyperfine structure parameters from [3,5] as starting points the fit routine converged well in all three transitions under study. The resulting line shapes as shown in Figure 4 accurately reproduce the patterns observed as well as the positions of the different hyperfine structure transitions. Severall runs of the fitting routine with distinctly different starting parameters led to similar results within less than one standard deviation. Reduced χ^2 values of about 2 were reached in the fitting routine, thus an uncertainty of 2σ is used for each parameter for further calculations. Except for the weakly contributing small B factors, all errors are well below 1 MHz. For all transitions the lorentzian and gaussian linewidth contributions to the Voigt profile of about 27(3) MHz and 21(2) MHz, respectively, were found to be equal within their experimental uncertainty and agree well with the results for the less abundant even isotopes. Particularly the A and B factors of each individual fine structure level, as extracted from the three different transitions, showed a perfect agreement with deviations of less than 0.5 MHz, confirming the numerical data analysis approach. To form final results, A and B factors from different transitions have been combined weighted with their individual errors.

A compilation of our results with earlier experimental and theoretical results is given in Table 1, covering the complete hyperfine structure of all 4p and 3d states. The 4p state A and B factors of [2] are confirmed with high precision, while the $A(^2P_{1/2})$ results from [6] are clearly ruled out. Theoretical predictions for A and B factors were calculated by extensive MBPT calculations for the 4s, 4p, and 3d-states. The approach includes all third order contributions for core polarization effects. In addition, correlation contributions were taken into account completely up to second order with inclusion of certain important higher order correlation effects, as discussed in detail in [5]. The results of these calculations for the A-factors have been revisited in [3] showing very good agreement with available experimental results for the 4s and 4p-states. A first result for the A(3d $^2D_{3/2}$) constant has been reported [4] while the corresponding B(3d $^2D_{3/2}$) factor is very unprecise and the remaining hyperfine structure constants of the 3d $^2D_{5/2}$ state have not been measured so far. In comparison to our set of experimental results, the theoretical MBPT expectations from [5] and [3] deviate less than 5% even in case of the small values of the 3d state hyperfine structure parameters of only a few MHz. This confirmation agrees well with the expected precision of the MBPT calculations and gives confidence into the modelling of the alkaline-like spectrum of Ca II by this technique. Furthermore, the improved calculations from [3] fit the experimental values slightly better than the earlier values from [5], except for A(4p $^2P_{3/2}$). In case of the large A(4p $^2P_{1/2}$) factor the precision of the theoretical prediction is as good as 0.5%. A second set of theoretical calculations from [16] show larger deviations of 8% for this A-factor, while the other A and B factors of the 4p configuration are also nicely reproduced. This generally good agreement between theory and experiment, with discrepancies in the prediction of the hyperfine structure parameters, which in no case exceeds 2 MHz, is a stringent test for both theory and experiment and imply the use of these precise results for metrological and quantum optical studies.

3.3 Isotope shifts of the even calcium isotopes

The isotope shift between two isotopes of masses A and A' is defined by $IS^{AA'} = \nu^{A'} - \nu^{A}$ and has a twofold origin: the change of the nuclear mass A and the change of the nuclear charge distribution. Thus the isotope shift is divided into two parts, the mass shift

$$\delta\nu^{\mathrm{MS}}_{AA'} = K^{\mathrm{MS}} \frac{M_{A'} - M_A}{M_A(M_{A'} + m_{\mathrm{e}})} \qquad (2)$$

Table 1. Hyperfine structure constants of the 3d $\rightarrow$ 4p transition of ^{43}Ca.

Author	$A(^2P_{1/2})$	$A(^2P_{3/2})$	$B(^2P_{3/2})$	$A(^2D_{3/2})$	$A(^2D_{5/2})$	$B(^2D_{3/2})$	$B(^2D_{5/2})$
this work	−145.4(0.1) MHz	−31.0(0.2) MHz	−6.9(1.7) MHz	−47.3(0.2) MHz	−3.8(0.6) MHz	−3.7(1.9) MHz	−3.9(6.0) MHz
[4] Exp.	−142 (8) MHz			−48.3(1.6) MHz		−0.5(6.0) MHz	
[6] Exp.	−158.0(3.3) MHz	−29.7(1.6) MHz					
[2] Exp.	−145.5(1.0) MHz	−31.9(0.2) MHz	−6.7(1.4) MHz				
[5] Theory	−148 MHz	−30.9 MHz	−6.3 MHz	−52 MHz	−5.2 MHz	−2.8 MHz[a]	−4.0 MHz[a]
[3] Theory	−144.8 MHz	−29.3 MHz		−49.4 MHz	−4.2 MHz		
[16] Theory	−135.7 MHz	−30.8 MHz	−6.0 MHz[a]				

[a] These values have been derived from the B/Q factors of [5,16] respectively, by using the tabulated quadrupole moment of $Q(^{43}\mathrm{Ca}) = -40.8$ (8) mb [17] disregarding a small Sternheimer correction.

and the field shift

$$\delta\nu^{\mathrm{FS}}_{AA'} = K^{\mathrm{FS}}\lambda_{AA'} \approx K^{\mathrm{FS}}\delta\langle r^2\rangle_{AA'}. \quad (3)$$

The field shift constant K^{FS} is given by

$$K^{\mathrm{FS}} = -4\pi\frac{Z}{6}\frac{e^2}{4\pi\epsilon_0}\Delta|\Psi(0)|^2 \quad (4)$$

where $\Delta|\Psi(0)|^2$ is the change in electron density at the nucleus between the lower and upper states in the transition. Contributions of higher order radial moments of the nuclear charge distribution are included in λ. As these corrections are very small for calcium ($\lambda/\delta\langle r^2\rangle \approx 0.996$ [18]) they can be neglected and the approximation given in equation (3) is very good. The mass shift is usually separated into the normal mass shift (NMS) due to the variation of the reduced electron mass and the specific mass shift (SMS) caused by a change of the correlation between the different electron momenta ($K^{\mathrm{MS}} = K^{\mathrm{NMS}} + K^{\mathrm{SMS}}$). While the normal mass shift constant K^{NMS} can easily be obtained from the transition frequency ν as $K^{\mathrm{NMS}} = m_{\mathrm{e}}\nu$, the specific mass shift constant $K^{\mathrm{SMS}} = \langle\sum_{i>j}\mathbf{p}_i\cdot\mathbf{p}_j\rangle/h$ is notoriously difficult to evaluate accurately because it is extremely sensitive to correlation effects. *Ab initio* calculations of isotope shift constants in Ca II have been carried out by single-configuration Dirac-Fock calculations [18] for the 4s $\rightarrow$ 4p transition and also by MBPT for other transitions [3,4].

For calculating the isotope shifts from our experimental data, the voltages of the resonance peak positions are converted to frequencies for each isotope and frequency differences from ^{40}Ca are extracted. The resulting isotope shifts for all stable isotopes are given in Table 2. The errors given are the sum of the statistical error from the fitting procedure and a systematical error, arising primarily from the uncertainty of about 1×10^{-4} in the acceleration potentials. The systematic uncertainty for the different isotopes are 2.0 MHz (^{42}Ca), 2.4 MHz (^{43}Ca), 2.9 MHz (^{44}Ca), 4.6 MHz (^{46}Ca), and 5.8 MHz (^{48}Ca) respectively. For comparison earlier experimental values obtained for the isotopes of mass 42, 43 and 44 by spectroscopy in an ion trap [20] are included in the table. For the even isotopes these values agree well within their rather large error bars, for the odd isotope ^{43}Ca a large discrepancy of about 250 to 300 MHz is observed. This deviation is ascribed to hyperfine pumping in case of the ion trap experiments and a resulting shift of the center of gravity which has only been taken into consideration in the corresponding data evaluation by somewhat artificially increasing the errors.

Within the accuracy of our measurement of about 10^{-3} the three transitions exhibit identical isotope shifts. Due to the closeness of the expected normal mass shift factors of $K^{\mathrm{NMS}}_{^2\mathrm{D}_{3/2}\rightarrow\,^2\mathrm{P}_{1/2}} = 189.81$ GHz amu, $K^{\mathrm{NMS}}_{^2\mathrm{D}_{3/2}\rightarrow\,^2\mathrm{P}_{3/2}} = 193.47$ GHz amu and $K^{\mathrm{NMS}}_{^2\mathrm{D}_{5/2}\rightarrow\,^2\mathrm{P}_{3/2}} = 192.48$ GHz amu this identity is also valid for the residual isotope shifts (RIS) evaluated by extracting the normal mass shift. Using a King plot [21] from the known mean square nuclear charge radii the field shift constants as well as the specific mass shift constants of the individual transitions have been determined. Two types of experimental data on nuclear charge radii do exist for calcium in literature: (1) absolute radii $\langle r^2\rangle$ extracted from combined analysis of electron scattering and muonic atom spectra [22] and (2) radii changes $\delta\langle r^2\rangle$ determined by optical isotope shifts [23].

Experimental data from both different approaches are combined to form a set of reliable accurate $\delta\langle r^2\rangle$ and $\langle r^2\rangle$ values for a long sequence of isotopes by Palmer *et al.* [1], and in a more recent publication by Nadjakov and Marinova [19]. The root mean square charge radii from [19] have been used to calculate the $\delta\langle r^2\rangle$ values for the King plot. These values are included in Table 2. The measured RIS values as well as the $\delta\langle r^2\rangle$ values calculated are "modified" by the factor $M_{40}M_A/(M_A - M_{40})$, to form the linear relation

$$\delta\nu^{\mathrm{RIS}}_{AA'}\frac{M_{40}M_A}{M_A - M_{40}} = K^{\mathrm{SMS}} + K^{\mathrm{FS}}\delta\langle r^2\rangle\frac{M_{40}M_A}{M_A - M_{40}}\cdot \quad (5)$$

In the King plot the "modified residual isotope shifts" are plotted as a function of the "modified mean square charge radii differences" and a linear regression can be performed with K^{SMS} given by the intersection point and K^{FS} given by the slope of the resulting line. The King plots of the different transitions are shown in Figure 5, the results of the linear regression are given in Table 3. The linear fit is perfect for the 3d $^2D_{3/2} \rightarrow$ 4p $^2P_{1/2}$ and 3d $^2D_{3/2} \rightarrow$ 4p $^2P_{3/2}$ transitions, the experimental

Table 2. Measured isotope shifts for the 3d $^2D_{3/2,5/2} \rightarrow$ 4p $^2P_{1/2,3/2}$ transitions in Ca II. $\delta\langle r^2\rangle$ values from [19] as used in the King plot are included.

A	Author	IS^{40,A} [MHz]			$\delta\langle r^2\rangle^{40,A}$
		$^2D_{3/2} \rightarrow ^2P_{1/2}$	$^2D_{3/2} \rightarrow ^2P_{3/2}$	$^2D_{5/2} \rightarrow ^2P_{3/2}$	[fm^2]
40		0	0	0	0
42	this work	−2353.4 (2.8)	−2352.2 (2.1)	−2350.4 (4.3)	0.2204 (7)
	[20]	−2366 (59)	−2359 (64)	−2272 (74)	
43	this work	−3464.3 (3.0)	−3462.4 (2.6)	−3465.4 (3.7)	0.1215 (4)
	[20]	−3163 (94)	−3243 (106)	−3187 (112)	
44	this work	−4501.8 (3.5)	−4498.7 (3.0)	−4495.2 (4.3)	0.2904 (10)
	[20]	−4509 (24)	−4538 (27)	−4510 (19)	
46	this work	-	-	−6477.8 (7.5)	0.1285 (4)
48	this work	−8301.3 (6.2)	−8297.7 (5.8)	−8287.8 (7.0)	0.00279 (1)

Table 3. Isotope shift constants of the 3d → 4p transitions in Ca II.

Transition	Author	$^2D_{3/2} \rightarrow ^2P_{1/2}$	$^2D_{3/2} \rightarrow ^2P_{3/2}$	$^2D_{5/2} \rightarrow ^2P_{3/2}$
K^{FS} [MHz/fm^2]	this work	79(4)	80(5)	78(12)
	[3]	88(3)		
	this work	−2179.6(4)	−2182.4(6)	−2180.0(1.1)
K^{SMS} [GHz amu]	[4][a]	−2191(23)	−2173(11)	−2161(19)

[a] Separation of field shift and specific mass shift was done by using the theoretical field shift constant K^{FS}_{3d}= + 110(1) MHz/fm^2 from [3,24].

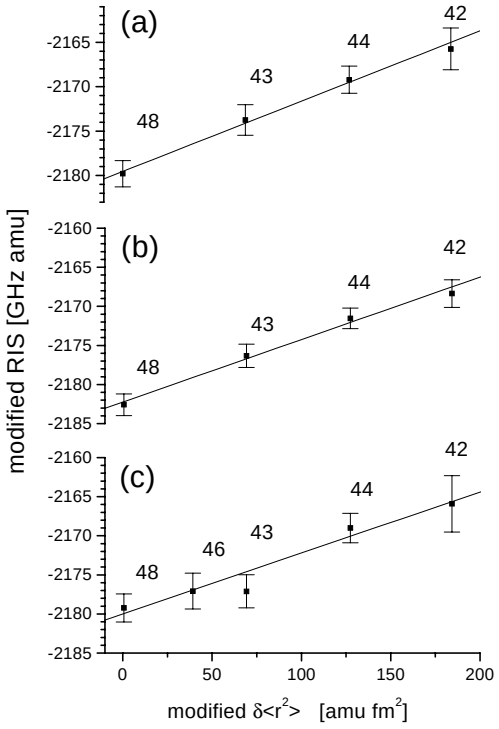

Fig. 5. "Modified residual isotope shifts" in the different 3d → 4p transitions ((a) 3d $^2D_{3/2} \rightarrow$ 4p $^2P_{1/2}$, (b) 3d $^2D_{3/2} \rightarrow$ 4p $^2P_{3/2}$, (c) 3d $^2D_{5/2} \rightarrow$ 4p $^2P_{3/2}$) *versus* "modified charge radii differences" from [19].

error bars are clearly overestimated due to cancellation of systematic errors. In the 3d $^2D_{5/2} \rightarrow$ 4p $^2P_{3/2}$ transition a deviation for the isotope ^{43}Ca by about the size of the error bar is observed. The reason for this small shift is not yet clearly understood. It could be due to a perturbing state, which affects one or more hyperfine structure components and which has not been taken into account in the hyperfine structure fitting procedure. As can be seen from Table 3 the field shift constants K^{FS} for the different transitions are equal within their uncertainties. A J-dependence of K^{FS} has been measured for the 5d states in Ba II [25], where it amounts to 5%. The dependence of this effect on the proton number Z leads to an expectation of less than 1% for the similar states of Ca II. Due to the large uncertainties of K^{FS} of about 7% (15% in the case of the 3d $^2D_{5/2} \rightarrow$ 4p $^2P_{3/2}$ transition due to bad statistics), this J dependence cannot be observed. In contrary, the errors of the specific mass shift constants are very small. As ^{40}Ca and ^{48}Ca have identical mean square charge radii the field shift between ^{48}Ca and ^{40}Ca vanishes completely. Thus K^{SMS} can be extracted precisely with an uncertainty of only 2×10^{-4}, increasing the precision in this number by about a factor of 20. For the specific mass shift no direct expectation for the J dependence does exist, but a contribution of about 1% can be assumed from the reference data from [4] in agreement with our results. Both results can be compared with theoretical expectations from the MBPT calculations [3,26]. The resulting field shift constant of K^{FS}_{3d} = +110(1) MHz/fm^2 for the 3d state is

rather large, indicating the relatively strong perturbation of the core *s* electrons by the valence d electron. The field shift constant of the 4p state ($K_{4p}^{FS} = +21.8(2)$ MHz/fm^2) is about five times smaller. A precision of about 1% for these numbers is expected. Combining these values we obtain a theoretical transition field shift constant of about 88(3) MHz/fm^2 in reasonable agreement with the average of the experimental field shifts of 79(4) MHz/fm^2. The discrepancy of about 10% only slightly exceeds the combined errors. It is ascribed to the *d*-electron perturbation of the core mentioned above or to higher order effects not fully included in these MBPT calculations. Nevertheless, its absolute value of only 9(6) MHz/fm^2 must be compared to the size of the 4s electron field shift of -261 MHz/fm^2, again underlining the high precision of recent MBPT calculations.

4 Summary

The ^{43}Ca hyperfine structure and the isotope shift for all stable isotopes of calcium have been measured for all three 3d $\rightarrow$ 4p transitions in Ca II by fast ion beam collinear laser spectroscopy. By fitting the hyperfine formula with assumed Voigt profiles to the experimental observed hyperfine patterns of ^{43}Ca, precise A and B hyperfine constants for upper and lower state were obtained. Experimental errors usually do not exceed 1 MHz. The A and B factors of the 3d $^2D_{5/2}$ state and the B factors of both 3d states have been measured for the first time. The other hyperfine structure results agree well with experimental data existing so far; they drastically increase the precision and thus permit a stringent test of the theoretical expectations achieved in the MBPT approach. The good agreement confirms the validity of this theoretical description. From the measured isotope shifts the specific mass shift and the field shift constants have been extracted by means of a King plot. Also these results are in good agreement with the theoretical MBPT predictions. The complete and precise knowledge of the hyperfine structure and isotope shifts in all low lying states of Ca II is seen as an ideal basis of the metrological and quantum optical studies in this alkali-like spectrum.

References

1. C.W.P. Palmer, P.E.G. Baird, S.A. Blundell, J.R. Brandenberger, C.J. Foot, D.N. Stacey, G.K. Woodgate, J. Phys. B **17**, 2197 (1984).
2. R.E. Silverans, L. Vermeeren, R. Neugart, P. Lievens, and the ISOLDE Collaboration, Z. Phys. D **18**, 352 (1991).
3. A.-M. Mårtensson-Pendrill, A. Ynnerman, H. Warston, L. Vermeeren, R.E. Silverans, A. Klein, R. Neugart, C. Schulz, P. Lievens and the ISOLDE Collaboration, Phys. Rev. A **45**, 4675 (1992).
4. F. Kurth, T. Gudjons, B. Hilbert, T. Reisinger, G. Werth, A.-M. Mårtensson-Pendrill, Z. Phys. D **34**, 227 (1995).
5. A.-M. Mårtensson-Pendrill, S. Salomonson, Phys. Rev. A **30**, 712 (1983).
6. A.T. Goble, S. Maleki, Phys. Rev. A **42**, 649 (1990).
7. F. Arbes, M. Benzing, Th. Gudjons, F. Kurth, G. Werth, Z. Phys. D **31**, 27 (1994).
8. R. Neugart, *Collinear fast-beam laser spectroscopy, Progress in Atomic Spectroscopy*, Vol. D (Plenum Press, 1987) p. 75.
9. A. Andl, K. Bekk, S. Göring, A. Hanser, G. Nowicki, H. Rebel, G. Schatz, R.C. Thompson, Phys. Rev. C **26**, 2194 (1982).
10. U. Klingbeil, J. Kowalski, F. Träger, H.-B. Wiegemann, G.z. Putlitz, Z. Phys. A **290**, 143 (1979).
11. E. Bergmann, P. Bopp, C. Dorsch, J. Kowalski, F. Träger, Z. Phys. A **294**, 319 (1980).
12. M. Arnold J. Kowalski, T. Stehlin, F. Träger, G. Zu Putlitz, Z. Phys. A **314**, 303 (1983).
13. C.-J. Lorenzen, K. Niemax, L.R. Pendrill, Phys. Rev. A **28**, 2051 (1983).
14. G.J. Beyer, E. Herrmann, A. Piotrowski, V.J. Raiko, H. Tyrroff, Nucl. Instr. Meth. **96**, 437 (1971).
15. H. Kopfermann, *Nuclear moments* (Academic Press, New York, 1958).
16. G.V. Meulebeke, Contribution à l'étude théorique des effects de la corrélation électronique en spectroscopie atomique, Dissertation, Université Libre de Bruxelles, Faculté des Sciences.
17. P. Pyykö, J. Li, J. Chem. Phys. **98**, 7152 (1993).
18. G. Torbohm, B. Fricke, A. Rosén, Phys. Rev. A **31**, 2038 (1985).
19. E.G. Nadjakov, K.P. Marinova, Atomic Data and Nuclear Data Tables **56**, 133 (1994).
20. W. Alt, M. Block, V. Schmidt, T. Nakamura, P. Seibert, X. Chu, G. Werth, J. Phys. B, **30**:L1 (1997).
21. W.H. King, *Isotope shifts in atomic spectra* (Plenum Press, New York and London, 1984).
22. H.D. Wohlfahrt, E.B. Scherqa, M.V. Hoehn, Y. Yamazaki, R.M. Steffen, Phys. Rev. C **23**, 533 (1981).
23. K. Heilig, A. Steudel, Atomic Data and Nuclear Data Tables **14**, 613 (1974).
24. P. Villemoes, A. Arnesen, F. Heijkenskjöld, A. Wännström, J. Phys. B **26**, 4289 (1994).
25. M. Van Hove , G. Borghs, P.D. Bisschop, R.E. Silverans, J. Phys. B **15**, 1805 (1982).
26. E. Lindroth, A.-M. Mårtensson-Pendrill, S. Salomonson, Phys. Rev. A **31**, 58 (1985).